

## University of Groningen

### Note

Ergincan, O.; Palasantzas, G.; Kooi, B. J.

*Published in:*  
Review of Scientific Instruments

*DOI:*  
[10.1063/1.4864195](https://doi.org/10.1063/1.4864195)

**IMPORTANT NOTE:** You are advised to consult the publisher's version (publisher's PDF) if you wish to cite from it. Please check the document version below.

*Document Version*  
Publisher's PDF, also known as Version of record

*Publication date:*  
2014

[Link to publication in University of Groningen/UMCG research database](#)

*Citation for published version (APA):*

Ergincan, O., Palasantzas, G., & Kooi, B. J. (2014). Note: Spring constant calibration of nanosurface-engineered atomic force microscopy cantilevers. *Review of Scientific Instruments*, 85(2), 026118-1-026118-3. [026118]. <https://doi.org/10.1063/1.4864195>

### Copyright

Other than for strictly personal use, it is not permitted to download or to forward/distribute the text or part of it without the consent of the author(s) and/or copyright holder(s), unless the work is under an open content license (like Creative Commons).

The publication may also be distributed here under the terms of Article 25fa of the Dutch Copyright Act, indicated by the "Taverne" license. More information can be found on the University of Groningen website: <https://www.rug.nl/library/open-access/self-archiving-pure/taverne-amendment>.

### Take-down policy

If you believe that this document breaches copyright please contact us providing details, and we will remove access to the work immediately and investigate your claim.

*Downloaded from the University of Groningen/UMCG research database (Pure): <http://www.rug.nl/research/portal>. For technical reasons the number of authors shown on this cover page is limited to 10 maximum.*

## Note: Spring constant calibration of nanosurface-engineered atomic force microscopy cantilevers

O. Ergincan,<sup>a)</sup> G. Palasantzas, and B. J. Kooi

*Nanostructured Materials and Interfaces Group, Zernike Institute for Advanced Materials, Nijenborgh 4, 9747 AG Groningen, The Netherlands*

(Received 22 October 2013; accepted 21 January 2014; published online 26 February 2014)

The determination of the dynamic spring constant ( $k_d$ ) of atomic force microscopy cantilevers is of crucial importance for converting cantilever deflection to accurate force data. Indeed, the non-destructive, fast, and accurate measurement method of the cantilever dynamic spring constant by Sader *et al.* [Rev. Sci. Instrum. **83**, 103705 (2012)] is confirmed here for plane geometry but surface modified cantilevers. It is found that the measured spring constants ( $k_{eff}$ , the dynamic one  $k_d$ ), and the calculated ( $k_{d,1}$ ) are in good agreement within less than 10% error. © 2014 AIP Publishing LLC. [<http://dx.doi.org/10.1063/1.4864195>]

The experimental determination of the spring constant ( $k$ ) of atomic force microscope (AFM) cantilevers plays an essential role in many AFM applications.<sup>1,2</sup> As a matter of fact, it is fundamentally important to calibrate the force sensing components to be able to convert cantilever deflection into an interaction surface force. So far, several calibration methods have been devised for this purpose. The three major approaches in these methods include: dimensional approach,<sup>3,4</sup> measuring the static deflection of the cantilever by applying/removing a known force,<sup>5,6</sup> and monitoring the dynamic response of the cantilever.<sup>7-9</sup> Nowadays, the ability to experimentally determine the spring constant of a microscopic component fast, relatively accurate ( $\sim 10\%$  level), and using a non-destructive technique is a significant challenge. The use of bulk material properties to determine the mechanical characteristics of microscopic components often significantly deviates (up to  $\sim 30\%$ ) from the calculated values due to the micro-fabrication techniques that produce structures with altered material properties.

Recently, Sader *et al.* presented a generalized model for acquiring the spring constant for similar plane geometry cantilevers independent of their dimensions, thicknesses, and material properties.<sup>10</sup> The method proposed by Sader *et al.* approaches the spring constant calibration problem by monitoring the response of the oscillating cantilever due to hydrodynamic loading in fluid (gas or liquid) environments. The latter requires measuring the Q-factor versus pressure  $P$  of a test cantilever, within the viscous regime, which has a similar plane view surface as the one for which the dynamic spring constant is required and properties are unknown.<sup>10,11</sup> Likewise, the radial frequency  $\omega_{test}$ , the length, and the width of the test cantilever are required for the dynamic spring constant calculation of the test cantilever. The generalized method for acquiring the dynamic spring constant  $k_d$  is given by the formula,<sup>10</sup>

$$k_d = \rho b^2 L \Lambda(\text{Re}) \omega_R^2 Q, \quad (1)$$

where  $\rho$  is the density of the fluid (gas or liquid) surrounding the cantilever,  $b$  and  $L$  are the cantilever width and length, respectively,  $\omega_R$  and  $Q$  are the radial resonant frequency and quality factor in fluid of the fundamental flexural mode, respectively.  $\text{Re} \equiv (\rho b^2 \omega_R)/4\mu$  is the normalized Reynolds number that indicates the importance of viscous forces relative to inertial forces in the fluid,<sup>12</sup> and  $\Lambda(\text{Re}) \approx a\text{Re}^{-0.7}$  is the dimensionless hydrodynamic function.<sup>10</sup>

Despite enormous progress so far, the desire for higher compositional resolution (minimum detectable mass) and high mass sensitivity (maximum frequency shift for a given mass change) is even today one of the major challenges. The latter is associated with the Q-factor, defined by the relation  $Q = 2\pi(E_{stor}/E_{dis})$  (ratio of stored to dissipated energy  $E_{dis}$  within an oscillation cycle). There are many groups working towards the fundamental limits of the cantilevers by re-designing and manufacturing cantilevers with minimum energy loss and high Q-factor.<sup>13-16</sup>

Moreover, advances in micro/nano manufacturing processes created a vast variety of probes, for example, coated with functional materials for mass detection of different components,<sup>17,18</sup> etched micro/nano grooves on the surfaces for fundamental studies of energy dissipation,<sup>19</sup> microfluidic flow experiments,<sup>20</sup> etc. All these studies require accurate spring constant calibration, clearly not only for smooth rectangular cantilevers, but also for ones with rough/corrugated surfaces.

However, up to now the experimental method by Sader *et al.*<sup>10</sup> to obtain the dynamic spring constant for cantilevers with corrugated/rough surfaces is missing. Therefore, in this paper we will study the validity of this method with systematic surface modifications of gold coated microcantilevers that are widely used in scanning probe technology. For this purpose, different length microcantilevers but with similar widths ( $\sim 30 \mu\text{m}$ ) and thicknesses ( $\sim 2 \mu\text{m}$ ) (see Table I) were modified by focused ion beam (FIB) along different etching directions as it is shown in Fig. 1.

The spring constant of each cantilever is measured before and after surface modification using the thermal tune calibration method (denoted by  $k_{eff}$  in Table I). The method

<sup>a)</sup> Author to whom correspondence should be addressed. Electronic mail: [orcunergincan@gmail.com](mailto:orcunergincan@gmail.com)

TABLE I. Properties of non-modified and modified microcantilevers. All symbols used are defined in the main text.

Type <sup>a</sup>	$f_{air}$ (kHz)	$Q_{air}$	$a$	$k_{eff}$ (N/m)	$k_d$ (N/m)	$k_{d,1}$ (N/m)
A-1	152.256	296	1.21	$5.80 \pm 0.58$	5.63	5.33
A-1(m)	153.257	287	1.12	$5.30 \pm 0.53$	4.93	5.22
A-2	134.528	266	1.14	$5.00 \pm 0.50$	5.56	4.08
A-2(m)	135.44	265	1.24	$4.60 \pm 0.46$	5.01	4.10
A-3	130.499	241	1.00	$3.60 \pm 0.36$	3.79	3.56
A-3(m)	132.974	234	0.90	$3.30 \pm 0.33$	3.38	3.54
B-1	326.214	452	0.84	$21.50 \pm 2.15$	23.26	20.40
B-1(m)	328.15	434	0.73	$21.20 \pm 2.12$	20.84	19.74
B-2	269.203	350	1.15	$11.40 \pm 1.14$	12.32	test
B-2(m)	271.57	359	1.03	$11.90 \pm 1.19$	13.89	12.77
B-3	272.049	360	0.84	$11.70 \pm 1.17$	12.24	12.84
B-3(m)	278.708	352	0.75	$11.50 \pm 1.15$	11.12	12.96

<sup>a</sup>(m) denotes modified cantilever.

is developed for the determination of  $k_{eff}$  measuring the cantilevers mechanical response due to agitations of impinging molecules from the surrounding fluid (ambient air, gases, liquids) and due to thermal dissipation via internal degrees of freedom with an accuracy down to  $\sim 10\%$ .<sup>21</sup> The AFM hardware measures the cantilevers fluctuations as a function of time from which, by Fourier transformation, the frequency dependent power spectral density (PSD) is acquired. Using the well-known Lorentzian function and equipartition theorem  $k_{eff}$  is acquired. Furthermore, the values of  $k_{eff}$  are depicted in Table I to compare with the dynamic spring constant results calculated via the hydrodynamic function.

The implementation of the dimensionless hydrodynamic function for the dynamic spring constant  $k_d$  calculation (Eq. (1)) relies on the fact that the energy dissipation of a resonator in the viscous regime is dominated by the hydrodynamic loading and requires information of the density, the viscosity of the fluid surrounding the cantilever, the width,

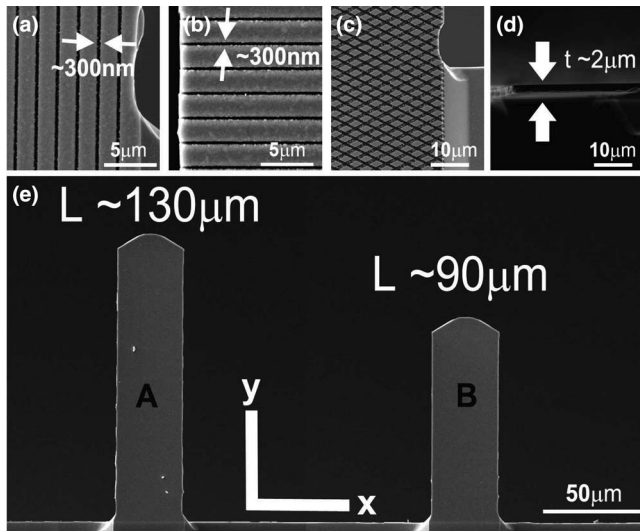


FIG. 1. SEM images of modified cantilevers (a) type (1), (b) type (2), (c) type (3), (e) SEM image of gold coated non-modified cantilevers of different lengths ( $\sim 130$  and  $\sim 90 \mu\text{m}$  denoted as A and B, respectively, similar widths ( $\sim 30 \mu\text{m}$ ), and thicknesses ( $\sim 2 \mu\text{m}$ ) as shown in (d).

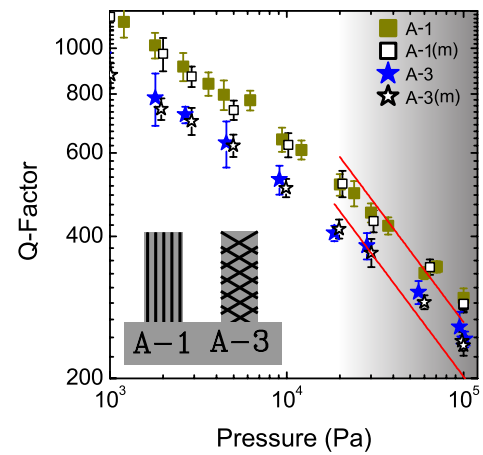


FIG. 2. Q-factor versus pressure  $P$  graph of cantilever A with dimensions as shown in Fig. 1 with surface modification types (1) and (3). “m” denotes modified cantilever. The red solid lines in the viscous regime ( $P > 10^4 \text{ Pa}$ ) show the typical  $Q \sim P^{-0.5}$  scaling behavior (illustrated with the gray gradient color).

the length, the resonance frequency, and the quality factor of the cantilevers. Accordingly, the dimensionless hydrodynamic function ( $\Lambda(\text{Re})$ ) scales with the energy dissipation into the fluid (gas or liquid).<sup>10</sup> Therefore, we performed noise measurements to determine the Q-factor as a function of vacuum pressure  $P$  (see Fig. S1 in the supplementary material<sup>22</sup>) as it is shown in Fig. 2. The experiments were conducted for cantilevers with two different lengths, denoted as A and B (Fig. 1(h)) (see Fig. S2 in the supplementary material<sup>22</sup>). They were modified using FIB (see Fig. S3 in the supplementary material<sup>22</sup>) in various etching directions: x and y are the coordinate notations of the cantilever surface plane (Fig. 1(e)). Etching in the y-direction (along the length of the cantilever, Fig. 1(a)) is denoted as (1), etching in the x-direction (along the width of the cantilever, Fig. 1(b)) is denoted as (2), and etching at 30 angles with respect to the y-direction, Fig. 1(c)), is denoted as (3). All grooves are  $2 \mu\text{m}$  apart from each other, while the etching depth is  $\sim 60 \text{ nm}$ . In addition, the dimensions of each cantilever were confirmed using a scanning electron microscope (SEM: Figs. 1(a)–1(d)). The hydrodynamic function is acquired for each modified and non-modified cantilever as shown in Fig. 3 (see Fig. S5 in the supplementary material<sup>22</sup>).

Utilizing  $\Lambda(\text{Re}) = a\text{Re}^{-0.7}$ , the “a” values of each individual cantilever before and after surface modification were collected from the fittings of the  $\Lambda(\text{Re})$  versus  $\text{Re}$  graphs (Fig. 3) as shown in Table I. Moreover, the dynamic spring constants  $k_d$  of each cantilever before and after surface modification (see Fig. S1 in the supplementary material<sup>22</sup>) were calculated using Eq. (1) and the “a” values from the fitting, see Table I.

Furthermore, Sader<sup>10</sup> proposed that “a” is a variable that only depends on the plan view geometry for the cantilevers with identical plan view dimensions. Thus, we obtain for the dynamic spring constant<sup>10</sup>

$$k_{d,1} = k_{d,\text{test}} \frac{Q}{Q_{\text{test}}} \left( \frac{f_R}{f_{R,\text{test}}} \right)^{2-\alpha}, \quad (2)$$

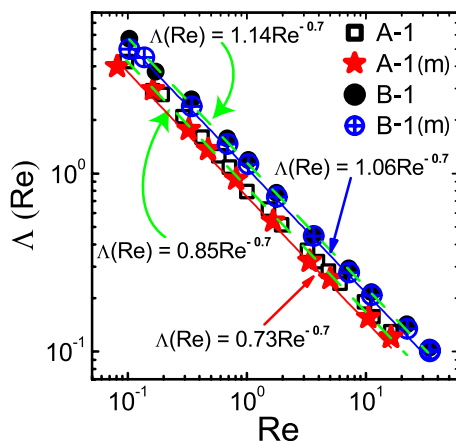


FIG. 3.  $\Lambda(\text{Re})$  vs  $\text{Re}$  graph of type (1) modification for cantilevers with dimensions A and B as shown in Fig. 1. “m” denotes the modified cantilever. The fittings with the green dashed lines correspond to the non-modified cantilevers A-1 and B-1. The solid red and blue fitting lines indicate the modified cantilevers A-1(m) and B-1(m), respectively.

where  $\alpha = 0.7$ , and the subscript “test” refers to the known parameters of the reference cantilever. Accordingly, both modified and non-modified cantilevers of the dimensions A and B have identical plan view geometries.<sup>10</sup> Therefore, we have calculated the values of  $k_{d,1}$  of both the modified and non-modified cantilevers using the  $k_d$  and the  $Q_{\text{air}}$  values of the sample B-2 (considered as a test cantilever). The values of  $k_{d,1}$  are given in Table I.

Despite the significant changes of the surface structures of the gold coated cantilevers, as Table I shows in detail, the dynamic spring constant  $k_d$  values are in a good agreement with the spring constant  $k_{\text{eff}}$  values acquired by the thermal tune method (within  $\sim 10\%$  error apart from sample B-2(m),  $\sim 17\%$  error). Furthermore, the spring constant  $k_{d,1}$  values calculated considering a non-modified cantilever, the B-2, as the test cantilever, are also in agreement with the spring constant values of  $k_{\text{eff}}$  and  $k_d$  (within  $\sim 10\%$  error apart from the samples A-2,  $\sim 18\%$  and B-3(m),  $\sim 13\%$  error).

In conclusion, from the analysis above it becomes evident that, for the cantilevers with modified surfaces, even if significant changes of the Q-factor take place in the intrinsic regime (see Fig. S7 in the supplementary material<sup>22</sup>), as the energy dissipation of a resonator in the viscous regime is dominated

by the hydrodynamic load, one can reliably and accurately obtain dynamic spring constant values from a test cantilever of the similar surface plane geometry, while the actual cantilever remains continuous in operation immersed within the fluid (gas or liquid) for which it is easy to acquire cantilever parameters such as resonance frequency and quality factor.

We would like to acknowledge financial support by the Dutch Technology Foundation (STW) under the Grant No. 10082.

- <sup>1</sup>R. Garcia and R. Perez, *Surf. Sci. Rep.* **47**, 197 (2002).
- <sup>2</sup>J. L. Arlett, J. R. Maloney, B. Gudlewski, M. Muluneh, and M. L. Roukes, *Nano Lett.* **6**, 1000 (2006).
- <sup>3</sup>J. Lubbe, L. Doering, and M. Reichling, *Meas. Sci. Technol.* **23**, 045401 (2012).
- <sup>4</sup>J. E. Sader and L. White, *J. Appl. Phys.* **74**, 1 (1993).
- <sup>5</sup>T. Senden and W. Ducker, *Langmuir* **10**, 1003 (1994).
- <sup>6</sup>C. T. Gibson, G. S. Watson, and S. Myhra, *Nanotechnology* **7**, 259 (1996).
- <sup>7</sup>J. P. Cleveland, S. Manne, D. Bocek, and P. K. Hansma, *Rev. Sci. Instrum.* **64**, 403 (1993).
- <sup>8</sup>J. E. Sader, J. W. M. Chon, and P. Mulvaney, *Rev. Sci. Instrum.* **70**, 3967 (1999).
- <sup>9</sup>A. D. Slattery, J. S. Quinton, and C. T. Gibson, *Nanotechnology* **23**, 285704 (2012).
- <sup>10</sup>J. E. Sader, J. A. Sanelli, B. D. Adamson, J. P. Monty, X. Wei, S. A. Crawford, J. R. Friend, I. Marusic, P. Mulvaney, and E. J. Bieske, *Rev. Sci. Instrum.* **83**, 103705 (2012).
- <sup>11</sup>J. E. Sader, J. Pacifico, C. P. Green, and P. Mulvaney, *J. Appl. Phys.* **97**, 124903 (2005).
- <sup>12</sup>J. E. Sader, *J. Appl. Phys.* **84**, 64 (1998).
- <sup>13</sup>K. Yasumura, T. Stowe, E. Chow, T. Pfafman, T. Kenny, B. Stipe, and D. Rugar, *J. Microelectromech. Syst.* **9**, 117 (2000).
- <sup>14</sup>P. Mohanty, D. A. Harrington, K. L. Ekinci, Y. T. Yang, M. J. Murphy, and M. L. Roukes, *Phys. Rev. B* **66**, 085416 (2002).
- <sup>15</sup>K. L. Ekinci, X. M. H. Huang, and M. L. Roukes, *Appl. Phys. Lett.* **84**, 4469 (2004).
- <sup>16</sup>O. Sahin, S. Magonov, C. Su, C. F. Quate, and O. Solgaard, *Nat. Nanotechnol.* **2**, 507 (2007).
- <sup>17</sup>N. V. Lavrik, M. J. Sepaniak, and P. G. Datskos, *Rev. Sci. Instrum.* **75**, 2229 (2004).
- <sup>18</sup>T. Braun, M. K. Ghatkesar, N. Backmann, W. Grange, P. Boulanger, L. Letellier, H.-P. Lang, A. Bietsch, C. Gerber, and M. Hegner, *Nat. Nanotechnol.* **4**, 179 (2009).
- <sup>19</sup>O. Ergincan, G. Palasantzas, and B. J. Kooi, *Phys. Rev. B* **85**, 205420 (2012).
- <sup>20</sup>N. Noeth, S. S. Keller, and A. Boisen, *J. Micromech. Microeng.* **21**, 015007 (2011).
- <sup>21</sup>B. Ohler, *Rev. Sci. Instrum.* **78**, 063701 (2007).
- <sup>22</sup>See supplementary material at <http://dx.doi.org/10.1063/1.4864195> for the sample dimensions, measurement setup, and extra figures.